

Intrinsic electrocaloric effects in ferroelectric poly(vinylidene fluoride-trifluoroethylene) copolymers: Roles of order of phase transition and stresses

B. Li,^{a)} W. J. Ren, X. W. Wang, H. Meng, X. G. Liu, Z. J. Wang, and Z. D. Zhang
 Shenyang National Laboratory for Materials Science, Institute of Metal Research,
 and International Centre for Materials Physics, Chinese Academy of Sciences, 72 Wenhua Road,
 Shenyang 110016, People's Republic of China

(Received 27 October 2009; accepted 14 February 2010; published online 9 March 2010)

The electrocaloric effects accompanied with the ferroelectric to paraelectric phase transitions in poly(vinylidene fluoride-trifluoroethylene) are investigated within the Landau–Devonshire theory. Just changing the nature of the phase transition from the first-order to the second-order reduces the isothermal entropy change, adiabatic temperature change and refrigerant capacity. The isothermal entropy change in the second-order transition is about one half of that in the first-order one, which is confirmed by experiments and is also consistent with the magnetocaloric counterpart. Converting to be film also leads to the reduction in electrocaloric effects, generally ascribed to the decrease of pyroelectric coefficients. © 2010 American Institute of Physics. [doi:10.1063/1.3353989]

Electrocaloric effect (ECE), a change of temperature induced by an electric field, provides an efficient and environment-friendly solution to cooling.^{1,2} Before the giant ECE with adiabatic temperature change of 12 K in $\text{PbZr}_{0.95}\text{Ti}_{0.05}\text{O}_3$ film was reported by Mischenko *et al.*³ in 2006, the magnitude of ECE had been too small to be of practical use. More recently, Neese *et al.*⁴ obtained large adiabatic temperature changes in poly(vinylidene fluoride-trifluoroethylene) [P(VDF-TrFE)] (55/45) (molar percentage, the same as below) copolymer and poly(vinylidene fluoride-trifluoroethylene-chlorofluoroethylene) tripolymer. Following these pioneer works, several ECE materials such as relaxor ferroelectric (FE) $0.9\text{PbMg}_{1/3}\text{Nb}_{2/3}\text{O}_3$ - 0.1PbTiO_3 and lead-free $\text{SrBi}_2\text{Ta}_2\text{O}_9$, have been reported.^{2,5,6} Meanwhile, Dunne *et al.*⁷ theoretically explained the origin of ECE for KH_2PO_4 and Lisenkov *et al.*⁸ calculated the ECE in $\text{Ba}_{0.5}\text{Sr}_{0.5}\text{TiO}_3$ from atomistic simulations. However, the theoretical investigation on ECE of P(VDF-TrFE), even through as a giant ECE material, has not been reported so far. In this letter, thereby, we use the Landau–Devonshire theory to investigate the influence of the order of phase transition on the ECEs in P(VDF-TrFE) polymers, which is believed to play a dominant role in magnetocaloric effect.⁹ Furthermore, comprehensive effects of stresses on the ECEs of the films are discussed in detail. Our results suggest that the order of phase transitions and the stresses play crucial roles in the ECEs.

For unconstrained and mechanically free samples, the thermodynamic potential can be expressed as the power series of polarization in terms of the Landau–Devonshire theory^{10–12}

$$G_{\text{bulk}} = G_0 + \frac{\alpha_0(T - T_0)}{2}P^2 + \frac{\beta}{4}P^4 + \frac{\gamma}{6}P^6 - EP. \quad (1)$$

Here, α_0 , β , and γ are the dielectric stiffness coefficients. E , P , and G_0 are electric field, polarization, and the free energy of paraelectric (PE) state in absence of applied electric fields,

respectively. For a thin film deposited on a substrate, the clamping effect from the substrate and the internal stresses arising from lattice and thermal expansion mismatches should be taken into account. Given the mechanical boundary conditions and the in-plane stresses, the thermodynamic potential of the thin film is modified as^{10–12}

$$G_{\text{film}} = G_0 + \frac{\alpha^*}{2}P^2 + \frac{\beta^*}{4}P^4 + \frac{\gamma}{6}P^6 + \frac{u^2}{s_{11} + s_{12}} - EP, \quad (2a)$$

$$\alpha^* = \alpha_0(T - T_0) - \frac{4Q_{13}u}{s_{11} + s_{12}}, \quad (2b)$$

$$\beta^* = \beta + \frac{4Q_{13}^2}{s_{11} + s_{12}}, \quad (2c)$$

where α^* and β^* are the renormalized dielectric stiffness coefficients, s_{11} , s_{12} the elastic compliances at constant polarization, Q_{13} the electrostrictive constant, u the misfit strains and T_0 Curie–Weiss temperature. The condition of equilibrium $\partial G / \partial P = 0$ yields the equations of state

$$E = \alpha_0(T - T_0)P + \beta P^3 + \gamma P^5, \quad (3a)$$

$$E = \alpha^*P + \beta^*P^3 + \gamma P^5. \quad (3b)$$

P - T curves at different applied electric fields and P - E loops at different temperatures can be derived from Eqs. (3a) or (3b). Substitution of $P(T, E)$ into Eqs. (1) or (2a) produces the free energy curves. In terms of $S = -(\partial G / \partial T)_E$, the excess entropy S^{EX} can be obtained. The isothermal entropy change induced by the change of electric field from E_1 to E_2 is determined by

$$\Delta S(T, \Delta E) = S^{\text{EX}}(T, E_2) - S^{\text{EX}}(T, E_1). \quad (4)$$

Similarly, the excess specific heat capacity of system relative to PE state in absence of applied electric fields, $\Delta C(T, E)$, can be derived. It should be noted that the whole procedure aforementioned is valid only for a reversible process. Such a method is also rational when high applied electric fields suppress a first-order transition (FOPT), by which hysteresis is

^{a)}Electronic mail: libing@imr.ac.cn.

TABLE I. Data for P(VDF-TrFE) copolymers.

Composition	65/35	55/45
Transition	FOPT ^a	SOPT ^c
T_0 (K)	313 ^a	341 ^c
α_0 (10^7 J m C ⁻² K ⁻¹)	3.5 ^a	2.4 ^c
β (10^{12} J m ⁻⁵ C ⁻⁴)	-1.5 ^a	0.39 ^c
γ (10^{14} J m ⁻⁹ C ⁻⁶)	1.9 ^a	...
s_{11} (10^{10} m ² N ⁻¹)	3.32 ^b	...
s_{12} (10^{10} m ² N ⁻¹)	-1.44 ^b	...
Q_{13} (m ⁴ C ⁻²)	3 ^c	...
C (10^3 J kg ⁻¹ K ⁻¹)	1.19 ^d	1.20 ^d
ρ (10^3 kg m ⁻³)	1.886 ^d	1.885 ^d

^aReference 13.^bReference 14.^cReference 15.^dReference 16.^eReference 4.

eliminated and C is defined at the transition point of the FOPT. Using the data listed in Table I,^{4,13–16} we calculated the ECE properties of P(VDF-TrFE) (65/35) and P(VDF-TrFE) (55/45).

The temperature dependencies of polarization for P(VDF-TrFE) (65/35) bulk are displayed in Fig. 1(a) at applied electric fields of 0 MV m⁻¹, and in Fig. 1(b) at 300, 320, 340, 360, 380, and 400 MV m⁻¹, respectively. The polymer experiences a FOPT from FE to PE state in absence of applied electric fields at $T_C=313$ K,¹³ while high applied electric fields drive the transition to higher temperatures and transform P - T curves to be continuous. We calculated hysteresis loops at 300 K for P(VDF-TrFE) (65/35) and P(VDF-TrFE) (55/45), respectively, as shown in Fig. 1(c). The polarization is saturated at an electric field of about 200 MV m⁻¹ for P(VDF-TrFE) (65/35). Therefore, we take 300 MV m⁻¹ as the initial electric field, E_i , to ensure a reversible process.

Figures 2(a) and 2(c) represent the excess specific heat capacity ΔC of system at applied electric fields of 300, 320, 340, 360, 380, and 400 MV m⁻¹, respectively. Suppression of the FOPT by high applied electric fields leads to a finite change of excess specific heat capacity at the phase transition, which accords with the change of P [Fig. 1(b)]. The applied electric fields shift the PE to FE transition to higher temperatures for P(VDF-TrFE) (65/35) rather than for

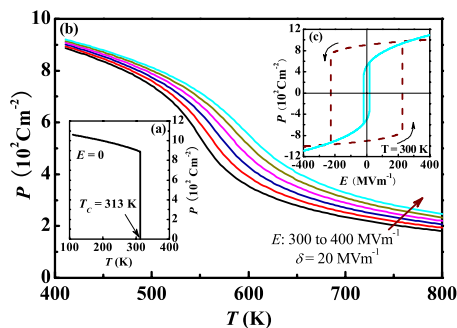


FIG. 1. (Color online) Temperature dependencies of polarization for P(VDF-TrFE) (65/35) bulk at zero field (a) where the arrow labels the T_C , and applied fields (b) where the step δ is 20 MV m⁻¹. The hysteresis loops at 300 K (c) with dashed line for P(VDF-TrFE) (65/35) and solid line for P(VDF-TrFE) (55/45), where the arrows mark the direction of electric-field changes.

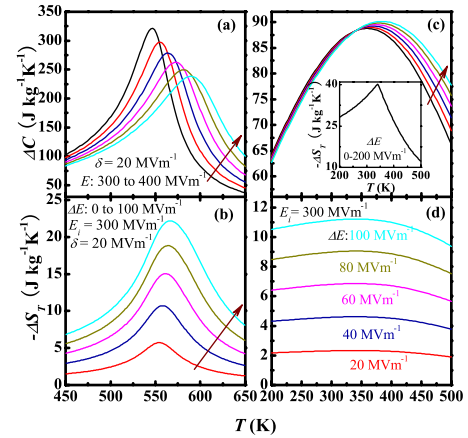


FIG. 2. (Color online) Temperature dependencies of excess specific heat capacity of system for bulk P(VDF-TrFE) (65/35) (a) and (55/45) (c). The temperature dependencies of isothermal entropy change for bulk P(VDF-TrFE) (65/35) (b) and (55/45) (d). The arrows indicate the electric field increasing and the step δ is 20 MV m⁻¹. Inset: the temperature dependence of isothermal entropy change for bulk P(VDF-TrFE) (55/45) at applied electric-field changes from 0 to 200 MV m⁻¹.

P(VDF-TrFE) (55/45). The variations in the isothermal entropy change with temperature are displayed in Fig. 2(b) for bulk P(VDF-TrFE) (65/35) and in Fig. 2(d) for P(VDF-TrFE) (55/45), respectively. Striking differences of ΔS_T - T curves are found for two polymers. The isothermal entropy change in P(VDF-TrFE) (55/45) is much less than that in P(VDF-TrFE) (65/35) at the same electric-field changes. The peaks of ΔS_T - T are surprisingly wide in P(VDF-TrFE) (55/45), which is the very characteristic for a second-order phase transition (SOPT). The difference of the ECEs should be ascribed to the order of the phase transition because the compositions of P(VDF-TrFE) (55/45) and (65/35) are very close and the FE properties except phase transitions are nearly identical with each other. At the transition point of a FOPT, there is a discontinuity of P , due to $P=(\partial G/\partial E)_T$, which appears as an infinite change of pyroelectric coefficient $p=(\partial P/\partial T)_E$. In a real material, even though it occurs over several Kelvin, a larger isothermal entropy change may be expected around a FOPT due to the steep change of polarization. By contrast, there is a moderate change of pyroelectric coefficient and a wider transition window for a SOPT owing to the nature of the continuous phase transition.

There is little hysteresis near the SOPT, as shown in Fig. 1(c). Thus, it is reasonable to neglect the effect of hysteresis on the ECE and calculate the isothermal entropy change of P(VDF-TrFE) (55/45) at the electric-field changes from 0 to 200 MV m⁻¹, which is presented in the inset of Fig. 2. The isothermal entropy change, 40 J kg⁻¹ K⁻¹, is basically consistent with the result of Neese *et al.*⁴ (50–60 J kg⁻¹ K⁻¹). The small difference may be ascribed to following two reasons: (i) the different samples may have different crystallinity (the films in the work of Neese *et al.*⁴ contain more than 25 wt % amorphous phase) and hence slightly different density (we use 1.889×10^3 kg m⁻³);¹⁶ (ii) the crystallization of amorphous phases will also contribute to the ECE.¹⁷

Figure 3 shows the differences of isothermal entropy change between the bulk and the films with misfit strains of 0.02, 0, -0.02 for P(VDF-TrFE) (65/35) at electric-field changes from 300 to 400 MV m⁻¹, respectively. It can be seen that the isothermal entropy change is reduced by trans-

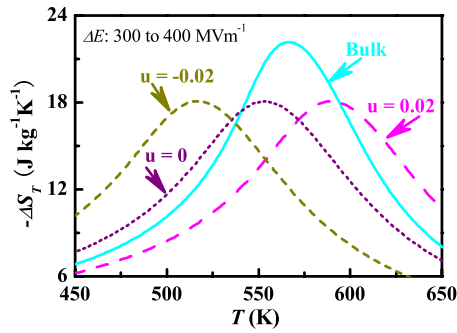


FIG. 3. (Color online) Temperature dependencies of isothermal entropy change for bulk P(VDF-TrFE) (65/35) and its films.

forming the bulk to the films, as found for BaTiO₃.¹⁶ For a partially clamped film where the top surface is free while the down surface is fixed on the substrate, if the pyroelectric axis is perpendicular to the surface of the film, the pyroelectric coefficient is represented as¹⁸

$$p^{\text{PC}} = p_3^X - \frac{2d_{31}\alpha_1}{s_{11} + s_{12}}, \quad (5)$$

p_3^X is the pyroelectric coefficient of the mechanically free sample (at constant stresses), d_{31} the piezoelectric constant, α_1 the thermal-expansion coefficient, s_{11} , s_{12} the elastic compliance constants. In most of pyroelectric materials, p^{PC} is less than p_3^X ,¹⁹ and hence the isothermal entropy change is reduced. However, the misfit strains in films only remarkably shift the peaks of $\Delta S_T - T$ (see Table II).

The adiabatic temperature change is evaluated by

$$\Delta T_{\text{ad}} = \frac{|\Delta S_T|^{\text{max}} \cdot T^{\text{max}}}{\rho C}. \quad (6)$$

Here, $|\Delta S_T|^{\text{max}}$ is the maximum of isothermal entropy changes, T^{max} the temperature where $|\Delta S_T|^{\text{max}}$ occurs, C the specific heat capacity, and ρ the density. Refrigerant capacity (RC) value is a measurement of how much heat can be transferred between the cold and hot sinks in an ideal refrigerant cycle. We calculate the RC values in terms of

$$\text{RC} = \int_{T^{\text{max}} - \frac{1}{2}\Delta T_{\text{ad}}}^{T^{\text{max}} + \frac{1}{2}\Delta T_{\text{ad}}} |\Delta S_T| dT. \quad (7)$$

For clarity, we summarize the ECE properties of P(VDF-TrFE) in Table II. It is obvious that $|\Delta S_T|^{\text{max}}$, ΔT_{ad} , and RC values in SOPT are much less than those in FOPT.

TABLE II. ECE properties of P(VDF-TrFE) copolymers (ΔE : 300 to 400 MV m⁻¹).

Composition	(65/35)				(55/45)
	Bulk	$u=0.02$	$u=0$	$u=-0.02$	
$ \Delta S_T ^{\text{max}}$ (J kg ⁻¹ K ⁻¹)	22	18	18	18	11
T^{max} (K)	566	590	553	516	342
ΔT_{ad} (K)	10.6	8.6	8.9	7.8	3.2
RC (J kg ⁻¹)	234	155	159	141	36

This result shows that when a ferroelectric with a FOPT has been saturated to avoid hysteresis, it is more advantageous than one with a SOPT. It is interesting that the isothermal entropy change in SOPT is about one half of that in FOPT, which is consistent with results in magnetocaloric effects.^{9,20} The result is also confirmed by the data of Nesse *et al.*,⁴ as follows: during the phase transition in the absence of the applied electric fields, the entropy change of P(VDF-TrFE) (55/45) is about 30 J kg⁻¹ K⁻¹, evaluated from the integral of C_p with respect to temperature in terms of $C_p - T$ curve in Figure S2 A of the work of Nesse *et al.*,⁴ while the entropy change is 56 J kg⁻¹ K⁻¹ for P(VDF-TrFE) (65/35).

To conclude, the order of the phase transitions and the stresses have significant effects on the ECEs in P(VDF-TrFE) polymers. FOPT results in twice larger isothermal entropy change than SOPT. Converting the polymers from bulk to film reduces the pyroelectric coefficient and thus leads to the reduction in ECEs.

This work has been supported by the National Basic Research Program of China (Grant No. 2010CB934603), Ministry of Science and Technology of China, the National Natural Science Foundation of China (Grant No. 50831006), and the Innovation Fund for Graduate Students of IMRCAS.

¹M. Lines and A. Glass, *Principles and Applications of Ferroelectrics and Related Materials* (Clarendon, Oxford, 1977).

²S. G. Lu and Q. M. Zhang, *Adv. Mater. (Weinheim, Ger.)* **21**, 1983 (2009).

³A. S. Mischenko, Q. Zhang, J. F. Scott, R. W. Whatmore, and N. D. Mathur, *Science* **311**, 1270 (2006).

⁴B. Neese, B. Chu, S. G. Lu, Y. Wang, E. Furman, and Q. M. Zhang, *Science* **321**, 821 (2008).

⁵A. S. Mischenko, Q. Zhang, R. W. Whatmore, J. F. Scott, and N. D. Mathur, *Appl. Phys. Lett.* **89**, 242912 (2006).

⁶H. Chen, T. L. Ren, X. M. Wu, Y. Yang, and L. T. Liu, *Appl. Phys. Lett.* **94**, 182902 (2009).

⁷L. J. Dunne, M. Valant, G. Manos, A. K. Axelsson, and N. Alford, *Appl. Phys. Lett.* **93**, 122906 (2008).

⁸S. Lisenkov and I. Ponomareva, *Phys. Rev. B* **80**, 140102(R) (2009).

⁹K. A. Gschneidner, Jr., V. K. Pecharsky, and A. O. Tsokol, *Rep. Prog. Phys.* **68**, 1479 (2005).

¹⁰N. A. Pertsev, A. G. Zembilgotov, and A. K. Tagantsev, *Phys. Rev. Lett.* **80**, 1988 (1998).

¹¹P. F. Liu, X. J. Meng, J. H. Chu, G. Geneste, and B. Dkhil, *J. Appl. Phys.* **105**, 114105 (2009).

¹²G. Akcay, S. P. Alpay, J. V. Mantese, and G. A. Rosetti, Jr., *Appl. Phys. Lett.* **90**, 252909 (2007).

¹³T. Furukawa, *Ferroelectrics* **57**, 63 (1984).

¹⁴H. Wang, Q. M. Zhang, L. E. Cross, and A. O. Sykes, *J. Appl. Phys.* **74**, 3394 (1993).

¹⁵Z. Y. Cheng, T. B. Xu, V. Bharti, S. X. Wang, and Q. M. Zhang, *Appl. Phys. Lett.* **74**, 1901 (1999).

¹⁶Y. W. Wong, N. M. Hui, E. L. Ong, H. L. W. Chan, and C. L. Choy, *J. Appl. Polym. Sci.* **89**, 3160 (2003).

¹⁷R. A. Anderson, R. G. Kepler, and R. R. Lagasse, *Ferroelectrics* **33**, 91 (1981).

¹⁸S. T. Liu, *Ferroelectrics* **22**, 709 (1978).

¹⁹F. Jona and G. Shirane, *Ferroelectric Crystal* (Pergamon, Oxford, 1962).

²⁰B. Li, W. J. Ren, Q. Zhang, X. K. Lv, X. G. Liu, H. Meng, J. Li, D. Li, and Z. D. Zhang, *Appl. Phys. Lett.* **95**, 172506 (2009).